Chirped fiber Bragg grating detonation velocity sensing

Cite as: Rev. Sci. Instrum. **84**, 015003 (2013); https://doi.org/10.1063/1.4774112
Submitted: 30 October 2012 . Accepted: 18 December 2012 . Published Online: 10 January 2013

G. Rodriguez, R. L. Sandberg, Q. McCulloch, S. I. Jackson, S. W. Vincent, and E. Udd

Chirped fiber Bragg grating detonation velocity sensing

G. Rodriguez,[1,a)] R. L. Sandberg,[1] Q. McCulloch,[1] S. I. Jackson,[2] S. W. Vincent,[2] and E. Udd[3]

[1]*Materials Physics and Applications Division, Los Alamos National Laboratory, Los Alamos, New Mexico 87545, USA*
[2]*Weapons Experiments Division, Los Alamos National Laboratory, Los Alamos, New Mexico 87545, USA*
[3]*Columbia Gorge Research, Fairview, Oregon 97024, USA*

(Received 30 October 2012; accepted 18 December 2012; published online 10 January 2013)

An all optical-fiber-based approach to measuring high explosive detonation front position and velocity is described. By measuring total light return using an incoherent light source reflected from a linearly chirped fiber Bragg grating sensor in contact with the explosive, dynamic mapping of the detonation front position and velocity versus time is obtained. We demonstrate two calibration procedures and provide several examples of detonation front measurements: PBX 9502 cylindrical rate stick, radial detonation front in PBX 9501, and PBX 9501 detonation along curved meridian line. In the cylindrical rate stick measurement, excellent agreement with complementary diagnostics (electrical pins and streak camera imaging) is achieved, demonstrating accuracy in the detonation front velocity to below the 0.3% level when compared to the results from the pin data. Finally, an estimate on the linear spatial and temporal resolution of the system shows that sub-mm and sub-μs levels are attainable with proper consideration of the recording speed, detection sensitivity, spectrum, and chirp properties of the grating. © *2013 American Institute of Physics*. [http://dx.doi.org/10.1063/1.4774112]

I. INTRODUCTION

In the performance characterization of high explosives (HE), the measurement of detonation wave speed is a fundamental quantity obtained through experimentation for comparison to equation-of-state models and hydrodynamic simulations that accurately predict detonation propagation, energy delivery, and timing in complex geometries (often with adjacent inert materials). These values are used to model the detonation evolution through a system along with subsequent detonation product and inert confiner motion.[1,2] For well over 50 years, elaborate methods have been used for measuring detonation and shock arrival positions including electrical shorting pins, ionization pins, piezoelectric gauges, and more recently fiber optic probes and microwave strip lines because of their reliability, time and position accuracy, and ease of use.[3–6] Yet they still retain certain drawbacks in their use that pertain to high voltage safety in proximity to high explosives, multiplexing recording channels, and discretization of data time signals when a continuous record is desired. From the standpoint of high explosive engineering and science, there still is a need for simple-to-field *in situ* probes that can continuously measure the dynamics (with sub-microsecond response times) of HE performance conditions. Additionally, these performance experiments need to be completed under critical geometries important for problems ranging from new formulation burn rates, surety engineering, initiation systems, to complex propagation in confined geometries with multiple material boundaries. Often HE performance – such as a detonation velocity or shock measurement – is done using surface probes (VISAR, photonic Doppler velocimetry (i.e., PDV), high speed optical camera imaging), discreet embedded gauges (pins, strain gauges), material density probes (x-rays, proton radiography), or low density flow fields with particle imaging velocimetry (i.e., PIV). Even the latest velocimetry PDV approaches using embedded fiber probes in explosives[7] require careful light collection matching using bare PDV single-mode fiber with a liquid waveguide surrounding the fiber that is buffered with a 1.6 mm diameter Teflon tube. In these probes, great care is taken to make sure the at the light rays reflected off the detonation front and collected by the embedded PDV probe are parallel to the detonation front propagation to prevent loss of return light signal. Additionally the large size of the embedded probe is also undesirable from a modeling perspective due to possible detonation flow disruption. On the other hand, embedded sensors based on single mode fiber Bragg gratings offer an attractive alternative due to their compact diameter size (~125 μm), flexibility in placement, and ease of use with standard recording equipment that is less stringent than PDV based systems. We believe this approach offers an attractive affordable alternative approach that complements other detonation front diagnostics. In this paper, we demonstrate an embedded fiber optic probe technique that is capable of *in situ* continuous recording of HE detonation burn front position and velocity with sub-μs temporal resolution, and with the flexibility to measure burn fronts along linear and curved surfaces.

Based on pioneering development work by Benterou and Udd *et al.*,[8–11] we explore the use of embedded fiber optic sensors using linearly chirped fiber Bragg gratings (CFBG) for detonation front measurement experiments under several HE geometries that demonstrate the technique's versatility. In this paper, we first describe the operating principle and system components. Next, we detail two CFBG calibration procedures[12,13] that one can use to measure detonation front position and velocity accurately to the percent level when

a)Electronic mail: rodrigeo@lanl.gov.

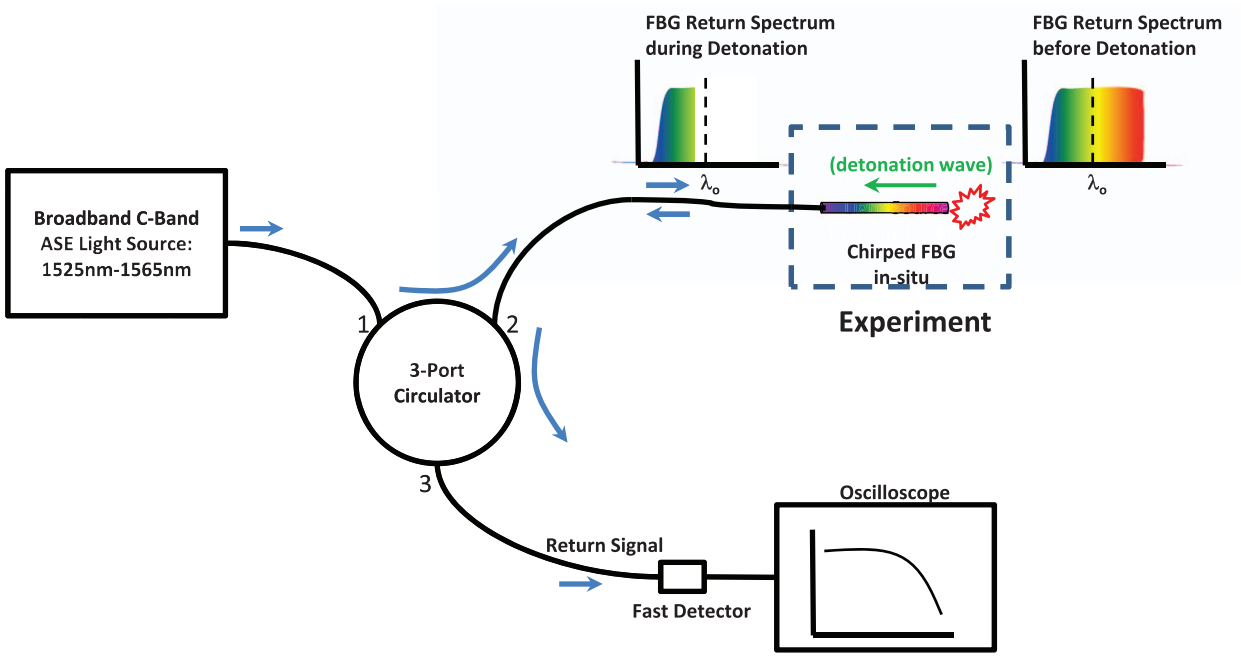

FIG. 1. Chirped fiber Bragg grating (CFBG) detonation velocity sensor system block diagram.

converting recorded data to position and velocity. We use three explosive geometries to demonstrate this ability: cylindrical rate stick, radial detonation front, and detonation along a curved meridian line of a hemispherical charge. In the cylindrical rate stick measurement, we validate CFBG burn front measurements by comparing the obtained velocities with those derived from well-established electrical pin and streak camera diagnostics.

II. SYSTEM OPERATION PRINCIPLE

As in case of photonic Doppler velocimetry sensors,[14,15] CFBG detonation velocity sensing also capitalizes on technology components developed for the fiber optic telecommunications industry. In Figure 1, we illustrate the operating principle of the system and describe each component below from source, to sensor, detection, and recording. Based on the first reported design and experimental principles developed by Benterou *et al.*,[8] we use an incoherent broadband amplified spontaneous emission (ASE) source centered about the well-known telecommunication C-band (1525 nm–1565 nm). Light from the ASE light source is launched into a single-mode fiber system to a 3-port power circulator. The power circulator directs light to the embedded CFBG sensor. The CFBG sensor consists of a linearly chirped grating written along a predetermined sectional length of bare SMF-28 with maximum reflectivity within the C-band. Detonation wave sensing is accomplished with the sensor by being in direct contact (embedded or surface) with the HE. As the HE detonation wave travels along the length of the sensor, the fiber's index of refraction is first modified by the intense shock driven into the fiber by the adjacent high-pressure detonation products as the wave propagates axially along the grating's length. In rapid succession, the grating is consumed by the high temperatures and pressures associated with this event. Shock-processed portions of the grating no longer reflect or transmit light due to substantial modification to the local index of refraction. Since spectral encoding of the CFBG wavelength reflection band is linear with length (linear chirp), propagation of a detonation axially along the fiber grating continually and linearly reduces the reflected grating bandwidth as a function of time. Thus, the detonation phase velocity along the fiber axis can be measured by a CFBG embedded in the HE or placed at various boundaries able to accommodate the bare 150-μm-diameter fiber (125 μm for cladding with 25 μm of recoating, typically polyamide). For these experiments, power levels launched into the CFBG detonation velocimetry system were typically 0.0 dBm (1 mW). Near complete total reflection (>90% light return) off the CFBG occurs along the detection leg of the system. After reflecting off the CFBG, the reflected light is directed through the power circulator at port 2, where only reflected light off the CFBG is detected at the circulator output port (port 3) using a fast (250 MHz BW) InGasAs photodetector. Dynamic recording of the event is done with a fast recording digitizing oscilloscope. The current bandwidth of the measurement system is limited by the response time of the photodiode.

In Figure 2, we graphically illustrate how a transformation from the experimentally recorded trace of voltage versus time at the detector is related to the length/position versus time response function of the grating after data reduction. The grating reflection bandwidth is centered at 1550 nm (Fig. 2(a)), but is less than the bandwidth of the ASE light source so that the flattest spectral portion of the ASE source overlaps with the grating reflectance band. In Figure 2(b), the reflected intensity, R, is proportional to the integrated return light spectrum off the grating. However, since encoding of grating length versus wavelength is linear, R is linearly proportional to L and λ, provided that the grating reflected spectrum produced by the ASE light source can be assumed to be an

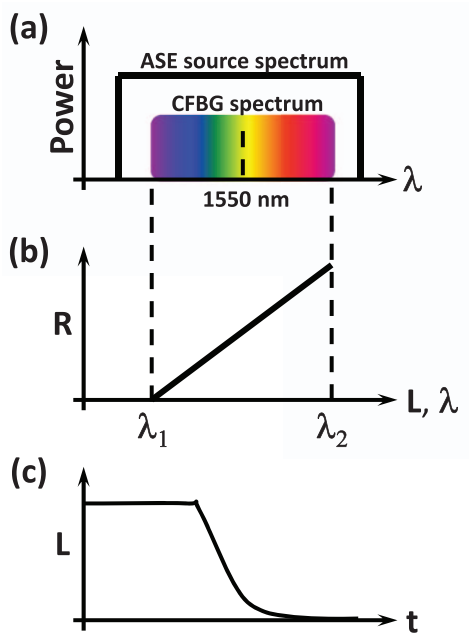

FIG. 2. Illustration of chirped fiber Bragg grating detonation velocity sensor system response functions. (a) CFBG spectrum is narrower than ASE light source spectrum. (b) Total reflected light intensity (R) varies linearly with grating length (L) and wavelength (λ) if both the source and return spectrums are idealized flat-tops. (c) A fiber adjacent to a detonating explosive will produce data that measures the detonation position (L) as a function of time.

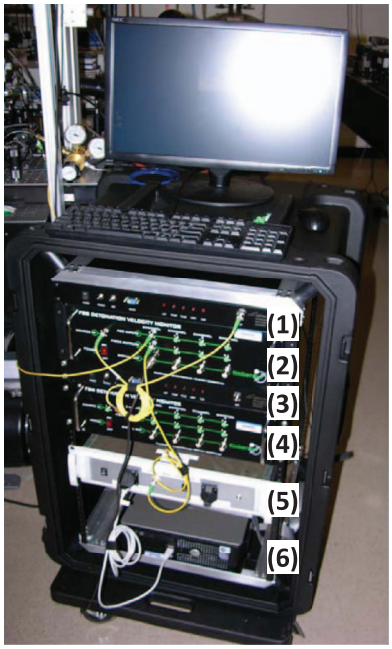

FIG. 3. Photograph of 8-channel chirped fiber Bragg grating detonation velocity detection system. Labeled components include: light sources (1) and (3); four-channel detector chassis (2) and (4); two-channel fiber spectrometer (5); personal computer (6). The recording digitizers are not shown.

idealized flat-top. In general, the integrated light return voltage signal is[8]

$$R(t) = a \int_{\lambda_1}^{\lambda_2(t)} S_G(\lambda)\,\mathrm{ASE}(\lambda)\,d\lambda, \qquad (1)$$

where, a is a normalization constant, $S_G(\lambda)$ is the grating reflection spectrum, ASE(λ) is the light source spectrum, and λ_1 and λ_2 are the lower and upper wavelength limits, respectively. Here, we assume λ_2 is the wavelength position where the detonation wave is located, i.e., $L(t) \propto R(t)$, and λ_1 corresponds to the shortest wavelength reflected by the grating, which is located nearest to the light source. Data analysis yields time-of-arrival data $L(t)$ for a detonation propagating along the CFBG sensor (Figure 2(c)). The temporal derivative of $L(t)$ computes the local detonation phase velocity along the fiber.

III. SYSTEM DESCRIPTION AND CALIBRATION

A. System description

The present experiments used a +17dBm Erbium based ASE light source (Lightwaves 2020, Inc. Model # EASEN171UA12897). The output was split using a 1 × 4 power splitter supporting up to 4 CFBG-sensor channels. Channel power upstream of the sensor is controlled via a variable attenuator and monitored using a four-channel light power meter (Eigenlight Corporation Model # A410-2-15). All channels were integrated into four-channel chassis boxes designed and built in collaboration with Timbercon, Inc. Each chassis box contains four three-port power circulators, four 10% power taps for spectral monitoring of the CFBG light return spectrum, and four dc-coupled, 50-Ω-output, 250-MHz InGaAs photodetectors. CFBGs connect to the chassis box that outputs electrical signals to a transient digitizer for recording. Typical recording bandwidth and sampling rates were 1 GHz and 5 GSamp/s, respectively. Typical input power to each channel of CFBG for sufficient light return recording level on the oscilloscope was 1 mW (0.0 dBm). A fiber-based 512-element linear-diode-array spectrometer (BaySpec Inc. Model # FBGA-IRS-1510-1590) was used to characterize the spectrum of each CFBG before experiments. Figure 3 shows a photograph of our rack-mounted portable detonation velocimetry system with eight channels. The portability of a rack-mounted system allows for ease of transportation to explosive firing sites, which are often located in remote and rugged environments.

B. CFBG details and calibration methods

The extraction of quality detonation velocity information is strongly dependent on the accuracy of the CFBG sensor power return versus length calibration. CFBG sensors come in a variety of lengths ranging from 10 mm to 100 mm depending on vendor availability and write methods (the two most common methods are phase mask UV laser write or direct femtosecond laser write). CFBGs in the present study were procured from multiple vendors (Timbercon Inc., O/E-Land Inc., and Micron Optics, Inc.) and consisted of germanium-doped fused-silica single-mode SMF-28 fiber. Typically, grating regions of SMF-28 bare fiber were chemically coated with a 25-μm-thick polyamide buffer layer for improved mechanical strength. Figure 4 shows a typical spectrum from an 85-mm-long CFBG. Note that the spectrum is not ideally flat topped, primarily due to the imperfect gain spectrum of our

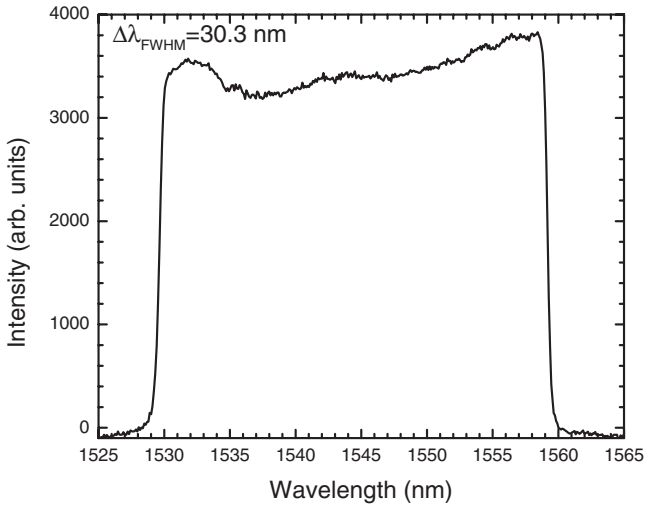

FIG. 4. Spectrum from an 85 mm chirped fiber Bragg grating. Bandwidth is $\Delta\lambda = 30.3$ nm.

Erbium ASE light source. The CFBG bandwidth $\Delta\lambda_{FWHM}$ in Figure 4 is 30.3 nm, which could be varied using a phase mask with an alternate phase delay slope (group delay or chirp).

Two calibration techniques were used in the present work to unfold reflectance signal verses axial position along the grating: laser cutting and laser heating. The "laser cut method" (method 1) calibrated CFBGs for detonation velocity sensing is accomplished by characterizing a single sacrificial grating out of a batch through a series of successive precision cuts along the grating length while measuring the signal output voltage versus cut position on the grating. It is then assumed that this calibration is the same for all other gratings in the batch that were written to equal manufacturing specifications. By measuring the voltage as a function of grating length, a one-to-one mapping from voltage to length can be applied to data from a detonation experiment to extract length versus time. This approach relies on the consistent signal return spectrum versus length calibration for the sacrificial CFBG and those fielded in experiments. Figure 5(a) shows a 3D wire grid surface plot of the light return intensity of an 85-mm long, 18-nm wide sacrificial CFBG versus wavelength and length position where cuts were made. Cutting was performed using a femtosecond laser machining setup[12,13] equipped with closed-loop motorized linear translation stages (Newport, Inc. Model XMS160) for positioning and rastering the cutting laser beam across the fiber in a saw-like fashion. The ultrafast laser system (Raydiance Inc. Discovery Model 03-500) was an 800-fs, 500-mW, 100-kHz repetition rate pulsed Erbium based fiber laser operating at 1552 nm. The beam was frequency doubled to 776 nm to improve energy deposition, and we used 4 μJ per pulse focused to a spot size of 8 μm to cut. The motorized linear translation x-y stages had a 10 nm unidirectional repeatability and an 80 nm bi-directional repeatability in position the fiber relative to the laser beam. In the z-direction (along the direction of the laser beam), the system had a $\sim$120$\times$ magnification (variable zoom) optical microscope/CMOS camera setup built into it to provide a telecentric view of the sample area to be machined that is collinear with the beam. We used this microscope to

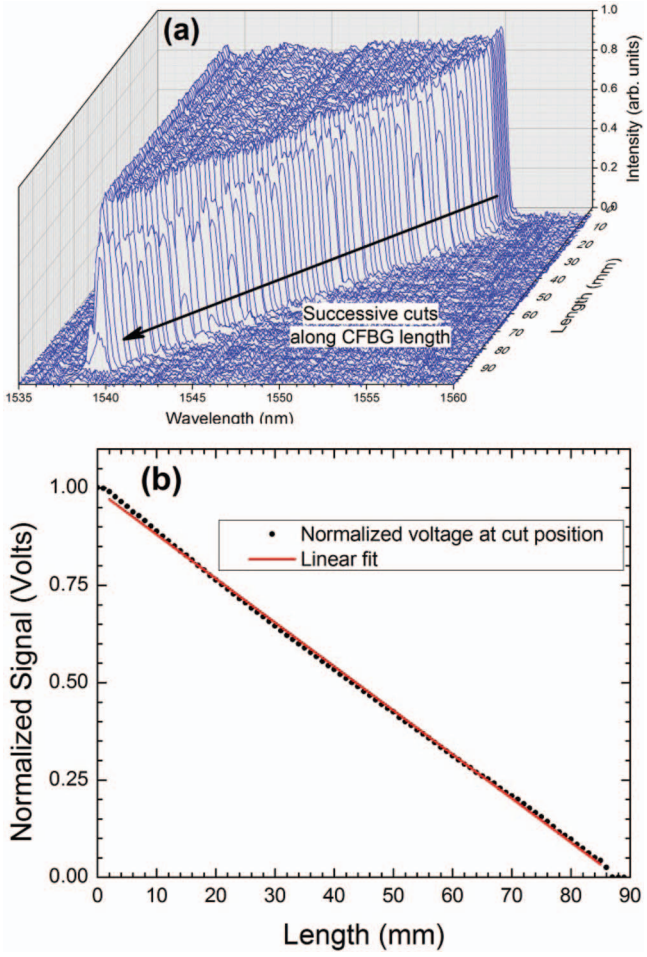

FIG. 5. Example of calibration method 1 showing successive 2 mm cuts of an 85 mm ($\Delta\lambda = 18$ nm) CFBG. In this the laser cut calibration method, a sacrificial CFBG is used. Plotted in (a) is a wire grid surface plot of grating spectrum versus wavelength and length that has been successively cut from beginning (long wavelength) to end (short wavelength) in 2 mm increments. Resulting measured voltage per cut position is shown in (b) as dots. The red solid line in (b) is a linear fit to data points and is used to unfold data from a detonation experiment by a mapping from voltage to length along the grating (slope is -0.011 V/mm).

position the fiber for cutting, and it provided cutting accuracy down to ± 2 μm.[12,13] Cut position increments along the length of the fiber were typically in 2 mm segments and are represented by each blue line trace in Figure 5(a). Simultaneous monitoring of the output voltage from our detector box and computer registered readout of the cut position from the laser system provides the desired mapping of voltage-to-length for calibration. The points in the plot of Figure 5(b) are the normalized dc voltages from the detector box as recorded by a voltmeter (50 Ω terminated) after each successive cut in 2 mm increments. The red trace in Figure 5(b) is used as an aid in demonstrating the linearity of the CFBG light return signal versus length. Slight deviations from linearity are attributed to spectral intensity non-uniformities (i.e., non-ideal flattop) in the CFBG.

A second "laser heat probe method" (method 2) individually calibrates each grating in a nondestructive fashion similar to the "hot tip probe" method used by Benterou *et al.*[8,9] Thus, while no CFBG is sacrificed, a calibration is needed for

each CFBG used. This approach relies on accurate measurement of the chirp (variation of the grating period/wavelength versus length) and grating length. Numerical integration of the measured spectrum using Eq. (1) computes a simulated light return signal. This yields a look-up-table (LUT) that relates simulated detector voltage to fiber position. The mapping of experimental voltage signal to fiber length is interpolated from the LUT. This calibration technique is superior to the laser-cutting approach because it accurately accounts for spectral intensity variation inherent in non-ideal flat-top CFBGs. We demonstrate this method by first showing how the chirp in the grating is measured. We use the same femtosecond laser machining setup from method 1 but reduce the power required for cutting by a factor of 10 and defocus the spot to about 100 μm. This allows us to only apply a localized, nondestructive heating to the fiber rather than a physical cut. The CFBG responds by producing a temporary "dip" in the return spectrum as shown in Figure 6(a). After laser removal, the CFBG cools and the reflectance spectrum returns to normal (i.e., no dip in spectrum). Proceeding in this manner, we step the laser heat probe along the CFBG length in successive 3-mm increments using the aforementioned linear translation stage. At each step, we recorded the spectrum and the laser heat probe position. CFBG chirp characteristics are thus determined from the spectral wavelength reading of the dips and the length position. Using this information, we numerically integrate the reflected-wavelength spectrum (black line, Fig. 6(b)) over wavelength/length to obtain the blue reflected-power data points. We then normalize and interpolated these data points using a bi-cubic spline to form a LUT (blue line, Fig. 6(b)). The LUT provides the required mapping from voltage to length in unfolding the data from a detonation experiment. This method of calibration accurately accounts for non-flat topped gratings as is apparent in the nonlinearity of the LUT curve for Fig. 6.

The CFBG detonation velocimetry and calibration techniques are demonstrated with phase-velocity measurements from three separate experimental geometries: outer wall velocity on a cylindrical rate stick, radially expanding detonation on a cylindrical charge surface, and detonation breakout along a meridian line on a hemispherical charge.

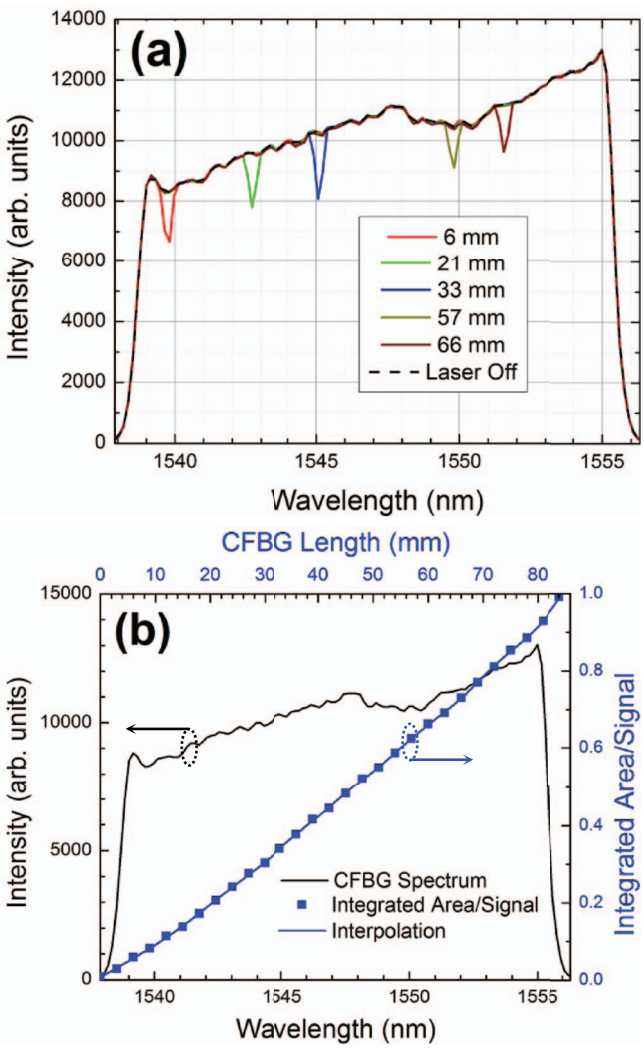

FIG. 6. Example of calibration method 2 by laser heat probe of an 85 mm ($\Delta\lambda = 18$ nm) CFBG. In the laser heat probe method the focused laser position is scanned along the length of the grating and to temporarily heat the grating. In the measured reflectance spectrum, a dip is formed at a given position by the laser heating shown in (a). The CFBG reflectance fully recovers when laser is turned off and the grating cools down. In (b), a collection of position points (blue squares) are used to numerically integrate the CFBG spectrum (black line) to compute the area under the spectrum and generate an interpolated look up table (LUT) (blue line) to be used in unfolding data from detonation experiments. In (b) the black line corresponds to bottom and left axes, and the blue symbols/line correspond to top and right axes.

IV. EXPERIMENTS

A. PBX 9502 rate stick

A cylindrical rate stick measurement of the insensitive HE PBX 9502 (95 wt. % TATB, 5 wt. % Kel-F 800) at room temperature was performed. The experimental geometry consisted of a 157.08-mm-long, 16.3-mm-diameter PBX 9502 cylindrical rod that was boosted by a 12.7-mm-diameter and 12.7-mm-long PBX 9407 booster pellet (94 wt. % RDX, 6 wt. % FPC461) and initiated by an RP-1 detonator (Teledyne RISI, Inc.) as shown in Fig. 7. The test was equipped with two CFBG fibers, electrical shorting pins, and a streak camera for detonation velocity determination. This provided proven diagnostics for discrete (pins) and continuous (streak) measurement to validate the CFBG data. Two 85-mm-long CFBG fibers were glued (M-Bond 200 epoxy) in direct contact along a 7.6-mm-wide facet polished into the charge outer diameter (orange shaded region in Fig. 7). A staggered pair of gratings was used since each individual grating was not long enough to span the entire rate-stick length. The end tips of the first and second CFBGs were placed 4.63 and 54.63 mm away from the upstream (initiation) end of the main PBX 9502 charge, respectively. Twelve time-of-arrival electrical shorting pins (Dynasen, Inc., Model CA-1038) were also fielded for comparison with the CFBGs. The pins were located 6.4, 18.85, 31.4, 43.76, 56.7, 69.48, 82.1, 94.92, 107.8, 120.7, 132.82, and 145.42 mm from the upstream end of the PBX 9502 charge. Finally, an imaging streak camera (Cordin Model 132) was used to record position of the detonation front versus time using an external light source to front illuminate the charge. The flat facet of the rate stick in between the CFBGs was

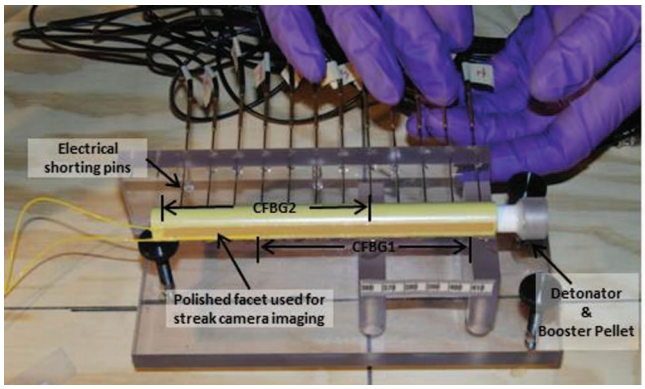

FIG. 7. Photograph of PBX 9502 rate stick assembly showing placement of diagnostics: two 85-mm-long CFBGs, 12 electrical pins, and the flat streak camera imaging facet.

polished to allow for specular light reflection from the charge surface. Light from an Argon flash source[16] was then reflected from the flat facet to the streak camera. The high-luminosity of the explosively driven Argon flash overwhelmed the light emission from the PBX 9502 reaction and product zones. Progression of the detonation along the charge first turns and subsequently destroys the polished facet surface. The destruction of the reflecting surface locally terminates light reflection to the camera, visualizing the detonation position versus time. Plotted in Figure 8(a) is the raw data as voltage traces as recorded by the CFBG sensors. The initial constant voltage signal for each probe indicates a period of time before detonation arrival at the grating that represents the total light return signal from the entire length of the grating. Immediately after detonation arrival at the probe, the signal decreases due to the near instantaneous index of refraction disruption caused by the interaction of the detonation burn front with the CFBG return light signal as described in Sec. II. Eventually, the full length of the CFBG is processed by the detonation and the reflected signal drops to zero. Processing of the data to obtain an L vs. t plot is accomplished by first normalizing the raw data signals to a full range between 0 and 1 V before applying a mapping transformation function to ordinate data points using the LUT calibration file (described in Sec. III B). This LUT is derived from "laser heat probe" method of calibration for each grating. Application of the LUT calibration file alters the shape and slope of the CFBG signals to account for spectral intensity curvature in the gratings. The curves before and after calibration are shown in Figure 8(b).

We compare the CFBG, pin, and streak data by plotting all results together. Figure 9(a) overlays the electrical pin, CFBG and streak camera data. The photograph in Figure 9(b) is a static (top) and dynamic position versus time streak (bottom) of the detonation along the charge. The inset table to Figure 9(a) shows the summary of the extracted velocity for all diagnostics (CFBGs, pins, streak camera) using a least-squares linear fit for each. The table shows that the CFBG results are within 0.3% of the data from the pins and streak camera. The standard error values in the slope of the linear fits reported as velocity in the table of Figure 9(a) are: ±0.0010, ±0.0011, ±0.0005, and ±0.021 mm/μs for CFBG1, CFBG2, streak camera, and pins, respectively.

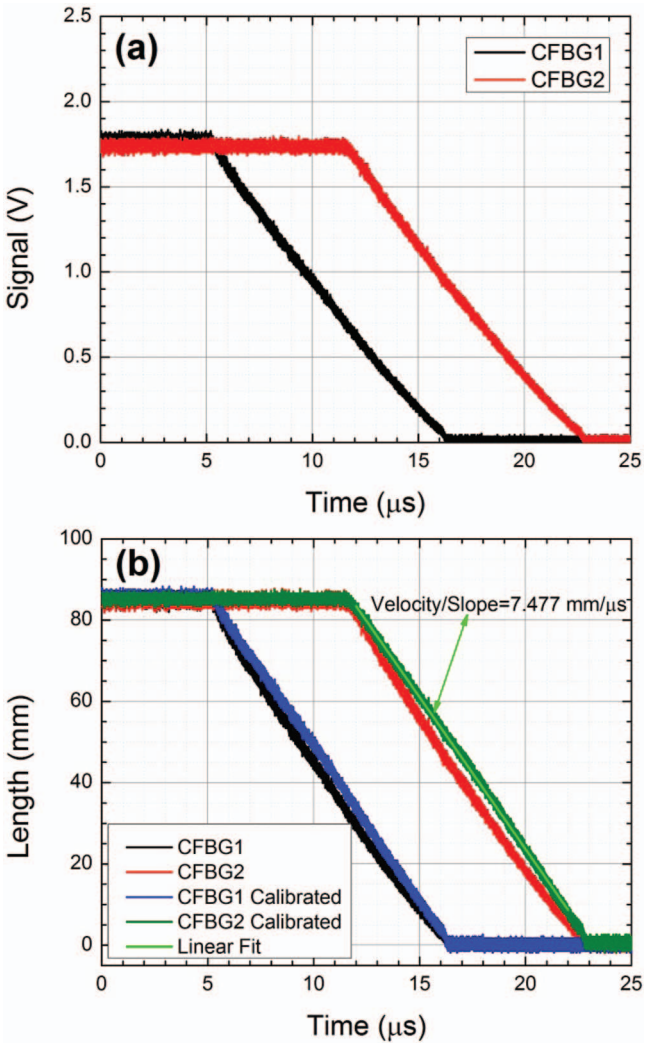

FIG. 8. Recorded CFBG data waveforms from PBX 9502 rate stick experiment: (a) raw data voltage versus time traces; (b) traces normalized and calibrated to length using LUT method of L vs. t data retrieval. A linear fit to the calibration corrected CFBG2 trace (green curve) in (b) yields a detonation front velocity (i.e., slope) of 7.477 mm/μs.

B. Radial detonation front in PBX 9501

For purposes of embedding CFBGs in structures that are not readily accessible or diagnosed by a surface measurement, detonation front wave speed measurements in confined geometries is also of interest. In Figure 10, we show a diagram and image for an experiment that produces a radial detonation front produced by initiation at the center of a circular shaped disk of PBX 9501 (95 wt. % HMX, 2.5 wt. % Estane, 2.5 wt. % BDNPA-F). The outer diameter of the shaped HE disk is 15.0 cm. In this experiment, three 60-mm-long CFBGs were glued into 76.2-μm wide by 177.8-μm deep machined recessed grooves that extend as radial spokes in a 25.4-mm-thick polycarbonate (Lexan) circular tamping plate. This tamping plate also contained the RP-1 detonator. All three CFBGs were separated by an azimuth angle of 120° and were offset from the center point of the tamping plate by 9 mm.

Figure 11 plots the data from the experiment. Figure 11(a) is a plot of the raw data for each of the three gratings fielded. The data in Figure 11(a) show some signal

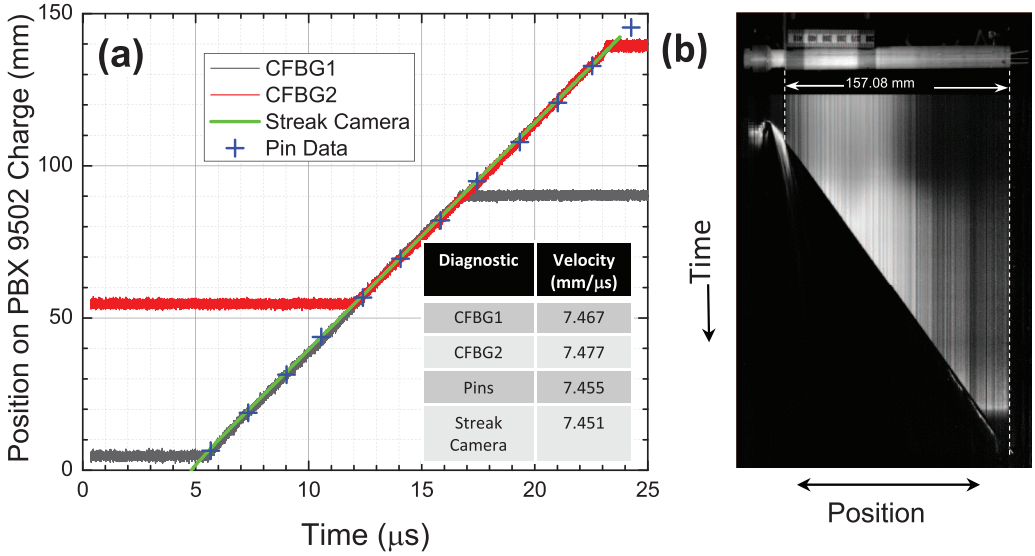

FIG. 9. (a) Results of the PBX 9502 rate stick experiment showing a comparison of the CFBG data (red and black curves), the streak camera break out data (green curve), and the electrical pin data (blue crosses). The inset table is the extracted velocity from a linear least squares fit for all three measurements: CFBGs, electrical pins, and streak camera. The standard error values in the slope of the linear fits reported as velocity in the table are: ±0.0010, ±0.0011, ±0.0005, and ±0.021 mm/μs for CFBG1, CFBG2, streak camera, and pins, respectively. (b) Images of the static (top) and dynamic (bottom) streak camera measurement.

fluctuations that appear during detonation propagation. We attribute these to micro-jetting from air gaps near the fiber where epoxy may not have sufficiently filled the fiber groove in the Lexan plate. Notwithstanding these gaps, simultaneity is excellent among the signals with all three CFBGs turning "on" within 15 ns and turning "off" within 100 ns. Upon normalization and calibration of the traces in Figure 11(a), we plot the results in Figure 11(b) using the "laser cut method" of calibration. The plotted traces show excellent symmetry and simultaneity in the radial front propagation. The average detonation front velocity measured by the CFBG diagnostic is 8.75 mm/μs, which compares well with the nominal detonation velocity of 8.8 mm/μs for PBX9501.[17] The 0.05 mm/μs deficit in the experimental measurement is likely due to the post-detonation flow divergence resulting in a lower than nominal detonation velocity for the radially expanding geometry.

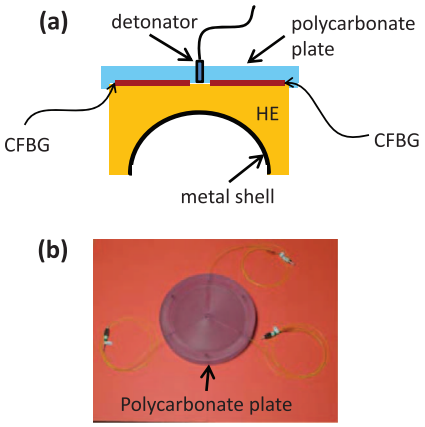

FIG. 10. Experimental diagram of (a) assembly side view and (b) photo of tamping plate showing location of CFBGs in radial detonation front measurement in conventional HE (PBX 9501). The CFBGs are each 60 mm long and are separated by 120° in azimuth angle.

C. PBX 9501 detonation along curved meridian line

In the final geometry presented, we demonstrate results from an experiment where the detonation front travels along a meridian line (longitude) in polar coordinates as initiated from the pole in a hemispheric-shaped PBX 9501 HE charge. The HE charge was tamped on the outside with a tantalum outer metal case, and the CFBGs on the experiment are in between the HE and case and exit the device near the equator. The fibers were laid in a 70-mm-long by 228.6-μm deep groove that was machined into the outer surface of the HE. They were epoxied (M-Bond 200) in place before the outer metal case was mounted in contact with the HE. An illustration of the placement of two CFBGs in the experiment is shown in Figure 12 showing a full azimuth angle between the gratings of 60°.

Figure 13 shows the results from this hemisphere experiment. The raw data plot in Figure 13(a) demonstrate the excellent simultaneous tracking of the detonation front by the two CFBGs, and the L vs. t plot of Figure 13(b) is derived by using the "laser cut method" of calibration as was shown in Figure 5 with excellent linearity between voltage signal versus length/wavelength. The measured detonation velocity in Figure 13(b) is not constant due to the interaction of the radially expanding detonation with the curved charge boundary at the meridian line from near the pole to the equator. To illustrate this point, the green trace in the plot of Figure 13(b) is a tangent line to a linear fit of the CFBG1 data between 5 μs and 7 μs and shows how the beginning and end of the CFBG1 data varies in slope from this tangent line. Figure 14 shows with local linear fits between 2.7 μs–5 μs (red), 5 μs–7 μs (green), and 2.7 μs–5 μs (orange) time slices that the apparent velocity in the front is increasing as the front travels over a recorded run of 70 mm: 8.83 mm/μs, 9.93 mm/μs, and 11.0 mm/μs, respectively. Further analysis on the detonation evolution in this system is beyond the scope of this paper.

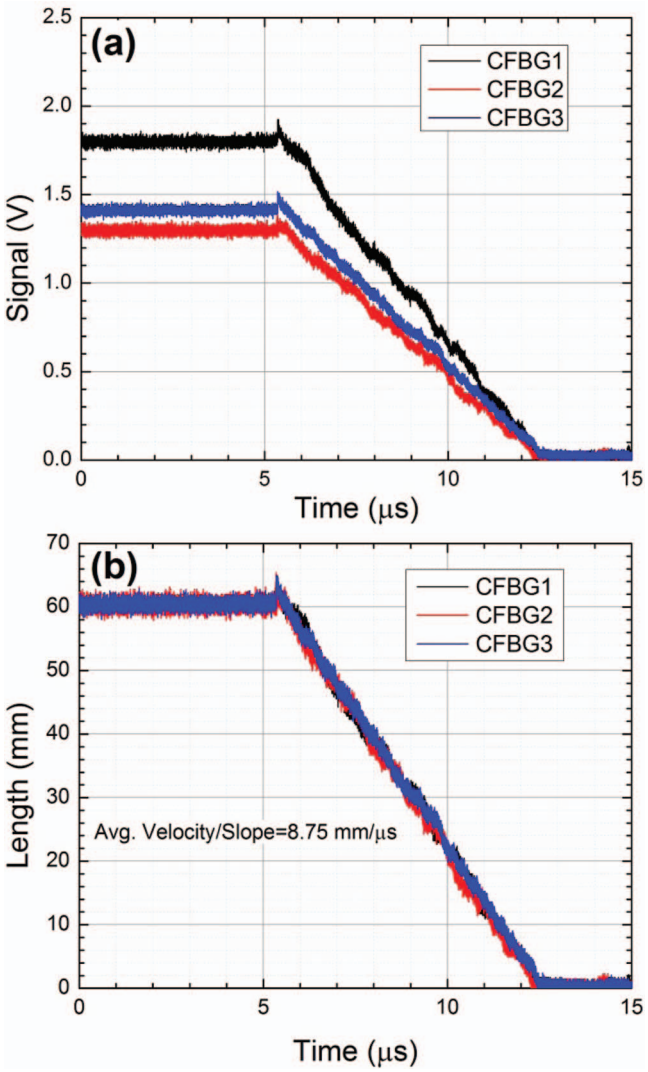

FIG. 11. Recorded CFBG data waveforms from PBX 9501 radial detonation front experiment: (a) raw data voltage versus time traces; (b) traces normalized and calibrated to length using "laser cut" method of L vs. t data retrieval. A linear fit to the calibrated traces in (b) yields an average detonation front velocity (i.e., slope) of 8.75 mm/μs.

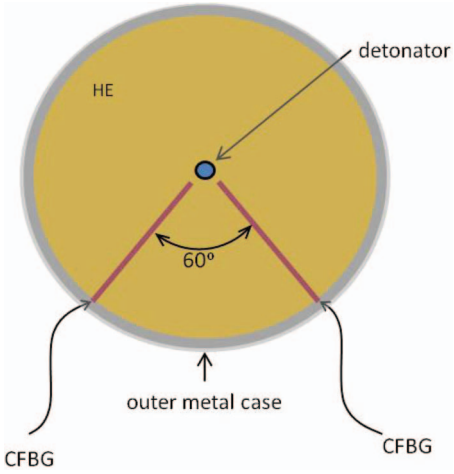

FIG. 12. Polar view of experimental diagram showing placement of CFBGs for detonation front measurement in PBX 9501 along a curved meridian (line of longitude). The hemispheric shaped HE charge is contained in an outer metal case, and two 70-mm-long CFBGs are epoxied between the HE and case. Azimuth angle between the two CFBGs is 60°.

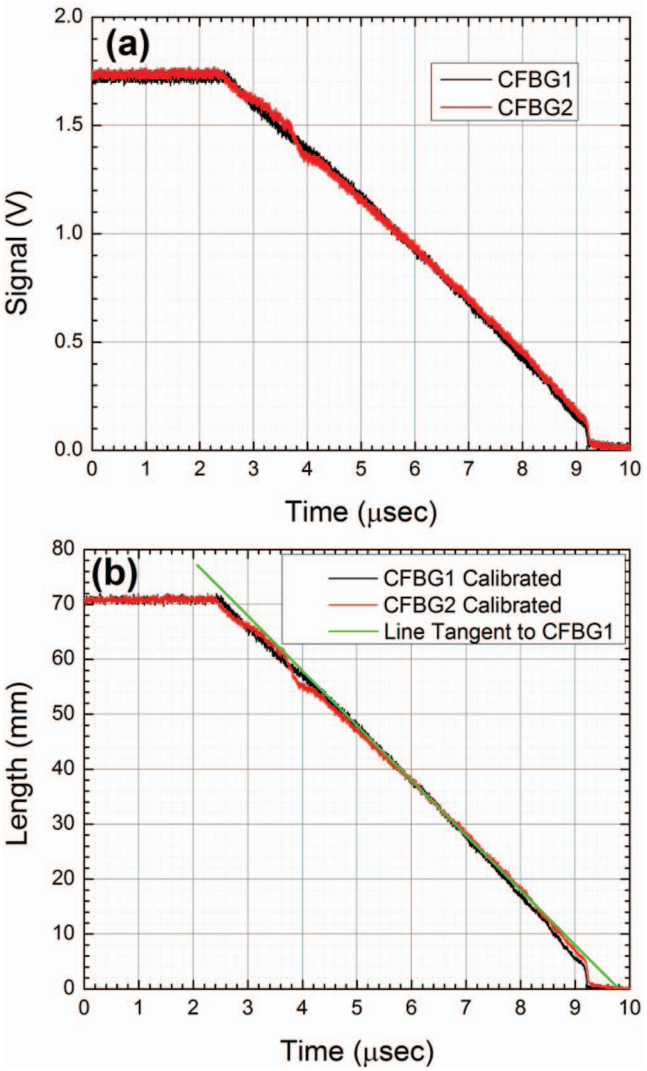

FIG. 13. Recorded CFBG data waveforms from PBX 9501 detonation front travels along a meridian line (longitude) in hemisphere detonation front experiment: (a) raw data voltage versus time traces; (b) traces normalized and calibrated to length using "laser cut" method of L vs. t data retrieval. The green trace represents an extrapolated line tangent to a linear fit of the CFBG1 calibrated trace between 5 μs and 7 μs. It is used to demonstrate that the phase velocity is not linear.

V. DISCUSSION

Section IV included results from several experimental configurations intended to demonstrate the versatility of the CFBG instrument at detecting detonation front motion with sub-microsecond temporal resolution over fairly long ($\geq$60 mm) detonation run distances and in differing geometric material boundaries. With some of the longest commercial CFBGs currently available at $\geq$100 mm and some of the shortest at $\leq$10 mm, a discussion on the spatial and temporal resolution afforded by the technology is warranted. Apart from the speed of photodiode detector and recording instrumentation bandwidth, the largest factor determining space and time resolution is the CFBG and its phase derivative or "chirp" ($d\lambda/dL$) as applied during the grating writing process. The chirp of the grating is the measure of wavelength change per unit length, which is most commonly a linear function for

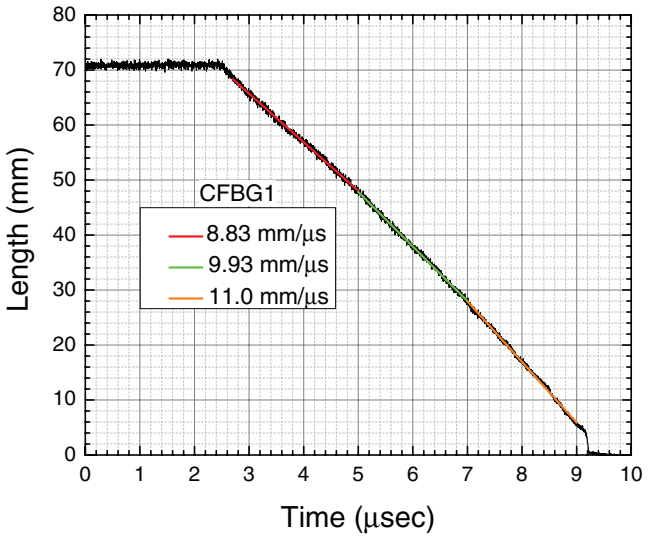

FIG. 14. Calculated velocity/slope fits to CFBG data from Fig. 13 show that curvature of hemispheric HE in experiment yields a phase velocity that increases with detonation front position as it propagates toward the equator.

telecommunications CFBGs. For example, a common telecommunications C-band grating can cover a wavelength range of 1530–1560 nm ($\Delta\lambda = 30$ nm) as shown in Figure 4. It is not unreasonable to expect the detection system to be sensitive to an intensity change below the percent level (see Figure 5(b)). This estimate is based on the approximate voltage change that could be resolved with 8-bit digitizers, where the voltage resolution may be improved using 12-bit digitizers. For the 85-mm-long CFBG shown in Figure 5(b) ($\Delta\lambda = 18$ nm), a 1% voltage change is approximately equal to a length change of $\Delta L = 0.91$ mm (as taken from voltage slope -0.11 V/mm in Fig. 5(b)). Therefore, an 85 mm CFBG with the spectrum shown in Figure 5 will have a relative spatial resolution of $\leq$0.9 mm. Similarly, 100-mm- and a 10-mm-long CFBGs can be expected to have $\sim$1 mm and $\sim$0.1 mm spatial resolution, respectively. For a detonation front traveling at 8.8 mm/μs (i.e., PBX 9501), this corresponds to a potential time resolution of 114 ns and 11.4 ns for CFBGs with a length of 100 mm and 10 mm, respectively, assuming comparable $\Delta\lambda$ bandwidths. For the results of the rate stick experiment in Figure 8, we computed the standard error in velocity based on inputting a variable temporal window length to the distance versus time records using a least squares fit. We observe that the fit velocity versus distance records produce a standard error that depends on window length size, and the sub-percent error level is achieved when window lengths are of 0.5–1.0 μs. This approach suggests a sub-μs time resolution for the rate stick data in Figure 8 and is consistent with the observed curvature for the meridian line experiment in Figure 13. Although the results in this paper demonstrate sub-μs level temporal resolution, experiments designed for rapid changes in detonation speed with sub-100 ns time resolution are in progress and is the subject of a future paper. Further improvements in resolution can be accomplished by increasing the spectral bandwidth ($\Delta\lambda \geq 30$ nm) of the CFBG or by increasing signal detection dynamic range using 12 bit type recording systems. This argument assumes that the full dynamic range of the digitizer is used and that the data are not limited by the signal-to-noise ratio. Some of these detailed resolution issues are a subject ongoing work, and the discussion here is to introduce the reader to these issues.

Two approaches for calibration of CFBGs were presented in Sec. III B. If all the CFBGs in a batch of fibers have nearly identical light return spectra, then method 1 ("laser cut method") should be adequate to obtain a voltage versus length calibration using a sacrificial CFBG for the batch lot. However, we believe the best approach for calibration is the non-destructive "laser heat probe method" (method 2) in which a voltage to length mapping is done using a numerically generated LUT for each CFBG. The results of our rate stick experiments clearly show that when a CFBG is non-ideal due to either the lack of flatness in the grating reflectance spectrum or in the light source output spectrum, a sufficiently accurate LUT can be generated to extract the L vs. t plot results. Out of convenience with an existing laser machining system in our laboratory, the laser heat method was used. Other scanning tip thermal probes can also be adequate at mapping out the grating chirp as was done with our laser heat probe.[8,9] A more sophisticated instrument such as an optical backscatter reflectometer (Luna Innovations, Inc.) is also capable of measuring CFBG length (to $<$10 μm) and chirp, but still must couple to measurements using a spectrometer and ASE light source for proper construction of the LUT.

VI. CONCLUSIONS

We have demonstrated a robust all optical fiber based approach to measuring high explosive detonation front position and velocity. Based on optical fiber technology developed for telecommunications at 1550 nm, light coupling of an erbium-based amplified spontaneous emission incoherent C-band light source into a single mode fiber probe with a chirped fiber Bragg grating was used to accurately track the detonation front. This detonation front position was tracked by measuring the interrupted light return signal as it propagated along the grating's length. Unfolding the detonation front position and speed from the recorded light return signal as a function of time requires an accurate calibration of the integrated light return signal as a function of the chirped fiber Bragg grating wavelength and physical length. We demonstrate two calibration procedures and provide several examples of detonation front measurements for a PBX 9502 cylindrical rate stick, a radially expanding detonation front in a disk shaped PBX 9501 charge, and detonation propagating along a curved meridian line in a PBX 9501 hemisphere. The conditions of these experiments demonstrate the system's versatility at successful measurement under conditions where material surface boundaries, in addition to the explosive, include contact with plastic and metal. In the cylindrical rate stick measurement, excellent agreement with established diagnostics (electrical pins and streak camera imaging) is achieved, demonstrating accuracy in the detonation velocity determination to below the 0.3% level with sub-μs temporal resolution. Finally, an estimate on the linear spatial and temporal resolution of the system show that sub-mm and sub-100 ns levels should be attainable in future experiments with proper consideration of

the grating spectrum and linear chirp properties. It is expected that these systems will play an increasing role in future detonation experimentation and high-speed diagnostics due to the continuous nature of the data record relative to discrete pin measurements and the fiber-based simplicity of the diagnostic system.

ACKNOWLEDGMENTS

Funding for this work was provided by the Gemini Project and the Campaign 2 "High Explosive Science" Program at Los Alamos National Laboratory under the auspices of the Department of Energy for Los Alamos National Security LLC under Contract No. DE-AC52-06NA25396. The authors also thank the Center for Integrated Nanotechnologies, Los Alamos National Laboratory for providing access to their ultrafast laser machining facility to cut and calibrate the fiber Bragg gratings used in this work. The authors also recognize M. Shinas of Los Alamos National Laboratory and V. Romero of National Security Technologies, Inc. for technical support on initial demonstration experiments. Also, M. Furlanetto of Los Alamos National Laboratory is acknowledged for program support under the Gemini Project at Los Alamos National Laboratory.

[1]J. B. Bdzil and D. S. Stewart, Phys. Fluids A **1**, 1261 (1989).
[2]D. E. Lambert, D. S. Stewart, S. Yoo, and B. L. Westcott, J. Fluid. Mech. **546**, 227 (2006).
[3]D. Bancroft, E. L. Peterson, and S. Minishall, J. Appl. Phys. **27**, 291 (1956).
[4]L. M. Barker, M. Shahinpoor, and L. C. Chhabildas, "Experimental diagnostics and techniques," in *High-Pressure Shock Compression of Solids* (Springer-Verlag, New York, 1993), pp. 43–73.
[5]G. E. Duvall, "Shock wave research: yesterday, today, and tomorrow," in *Shock Waves in Condensed Matter* (Plenum, New York, 1986), pp. 1–12.
[6]G. H. McCall, W. L. Bongianni, and G. A. Miranda, Rev. Sci. Instrum. **56**(8), 1612 (1985).
[7]O. Strand, D. Hare, R. Garza, T. Whitworth, and D. Holtkamp, in *Proceedings of the 14th International Detonation Symposium, Coeur d'Alene, 2010* (Office of Naval Research, Arlington, VA, 2010), p. 401.
[8]J. Benterou, C. V. Bennett, G. Cole, D. E. Hare, C. May, E. Udd, S. J. Mihailov, and P. Lu, Proc. SPIE **7316**, 73160E (2009).
[9]E. Udd, J. Benterou, C. May, S. J. Mihailov, and P. Lu, Proc. SPIE **7677**, 76770B (2010).
[10]E. Udd, in *Proceedings of Joint Army-Navy-NASA-Air Force, San Antonio, 2012* (Chemical Propulsion Information Agency Center, Columbia, MD, 2012).
[11]E. Udd and J. Benterou, Proc. SPIE **8370**, 83700L (2012).
[12]Q. McCulloch, A. M. Dattelbaum, G. Rodriguez, R. L. Sandberg, and K. W. Staggs, in *Lasers, Sources, and Related Photonic Devices*, OSA Technical Digest (CD) (Optical Society of America, Washington, DC, 2012), paper JTh2A.24.
[13]R. L. Sandberg, Q. McCullouch, A. M. Dattelbaum, K. W. Staggs, and G. Rodriguez, in *Conference on Lasers and Electro-Optics (CLEO): Applications and Technology*, OSA Technical Digest (online) (Optical Society of America, Washington, DC, 2012), paper AW3J.2.
[14]O. T. Strand, D. R. Goosman, C. Martinez, T. L. Whitworth, and W. W. Kuhlow, Rev. Sci. Instrum. **77**, 083108 (2006).
[15]A. R. Valenzuela, G. Rodriguez, S. A. Clarke, and K. A. Thomas, Rev. Sci. Instrum. **78**, 013101 (2007).
[16]W. C. Davis, T. R. Salyer, S. I. Jackson, and T. D. Aslam, in *Proceedings of the 13th International Detonation Symposium, Norfolk, 2006* (Office of Naval Research, Arlington, VA, 2006), p. 1035.
[17]T. R. Gibbs and A. Popolato, *LASL Explosive Property Data (Los Alamos Scientific Laboratory Series on Dynamic Material Properties)* (University of California, Berkeley, 1980).